Microfireballs in Stratified Target Chamber Gases in the Light Ion Target Development Facility - Final Report for the Period September 9, 1983 to September 30, 1985

T.J. Bartel, G.A. Moses and R.R. Peterson

September 1985

UWFDM-677

FUSION TECHNOLOGY INSTITUTE

UNIVERSITY OF WISCONSIN

MADISON WISCONSIN

Microfireballs in Stratified Target Chamber Gases in the Light Ion Target Development Facility - Final Report for the Period September 9, 1983 to September 30, 1985

T.J. Bartel, G.A. Moses and R.R. Peterson

Fusion Technology Institute
University of Wisconsin
1500 Engineering Drive
Madison, WI 53706

http://fti.neep.wisc.edu

September 1985

UWFDM-677

DOE/DP/40184-1

MICROFIREBALLS IN STRATIFIED TARGET CHAMBER GASES IN THE LIGHT ION TARGET DEVELOPMENT FACILITY

Final Report for the Period September 9, 1983 to September 30, 1985

T.J. Bartel

G.A. Moses

R.R. Peterson

Department of Nuclear Engineering
Fusion Technology Institute
University of Wisconsin-Madison
Madison, Wisconsin 53706-1687

September 1985

UWFDM-677

Work Performed Under Contract DE-AS08-83DP40184 with the U.S. Department of Energy.

Abstract

The fireball emanating from the microexplosion of an inertial confinement fusion (ICF) target in the light ion fusion Target Development Facility (TDF) may possibly be directed away from critical components by the presence of a target chamber nonuniform gas. Using a two-dimensional Eulerian hydrodynamics computer code, we have simulated the behavior of a microfireball in a nitrogen gas that is covered with a layer of helium. An increased reduction in the shock strength in the nitrogen is seen as the interface between the nitrogen and helium is closer to the point where the target explodes.

An investigation was made to determine if the use of multiple layered cavity gases with different opacities could reduce the overpressure on the diodes or on diagnostic equipment placed below the target in a light ion beam chamber. Figure 1 illustrates the geometry under consideration. The target chamber was taken as a right circular cylinder. The cavity gases were then segregated into the two regions as illustrated; the top region would contain an optically transparent gas. The hypothesis is that once the radiation front of the fireball has reached the gas interface, "venting" of the radiation upward would then result in a nonspherical hydrodynamic expansion of the fireball in region B and thus reduce the pressure loading in the radial and downward axial directions.[1]

To test this theory, a 2-D Eulerian radiation fluid dynamics computer code was written.[2] The 2-T diffusion approximation[3] was used for modeling the radiation field. This assumption is valid in the lower cavity gas (region B) but is incorrect for the upper gas due to its low opacity. However, since we were not interested in modeling the behavior of the fireball in this region, the diffusion model was sufficient to obtain realistic boundary conditions for the lower gas region. The ramifications of this approximation will be discussed later. A tabular equation of state was used for the lower gas;[4] the upper gas was modeled as optically transparent.

1. Calculations

The present analysis used helium as the transparent gas (region A) and nitrogen as the "cavity" gas (region B). The calculations were done in cylindrical geometry using 5 cm square computational meshes. The radius was taken as 250 cm with a no-flow boundary. The axial "top" and "bottom" were modeled as free-flow boundaries. Typically the region below the target was 250 cm and

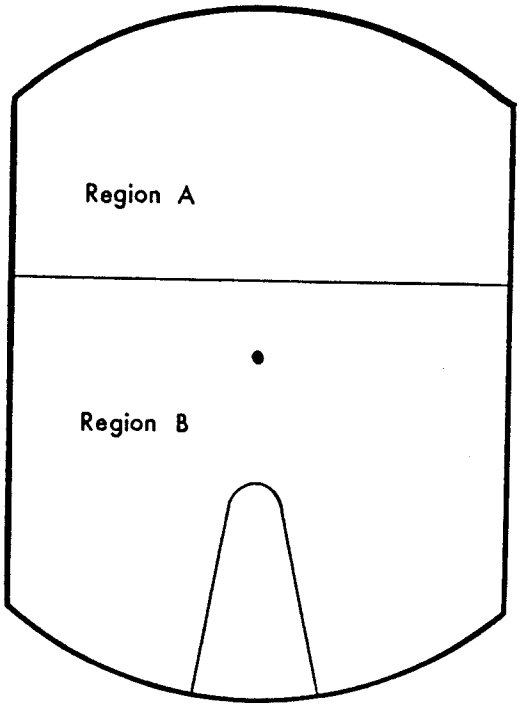

Fig. 1 TDF Cavity

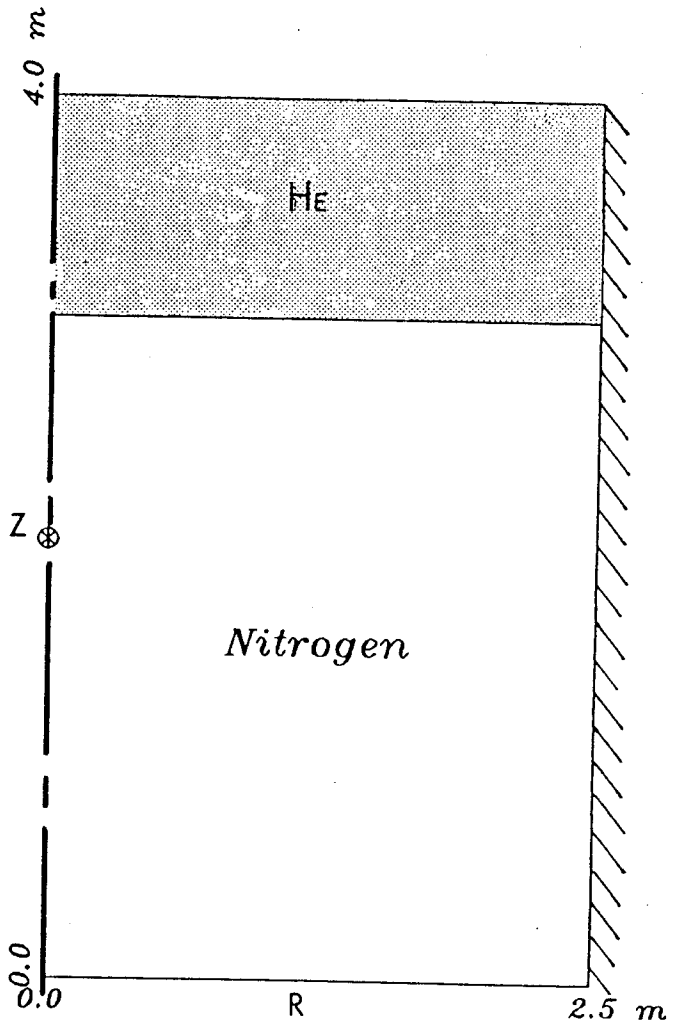

Fig. 2 Typical Computational Domain (100 cm. case)

the He region 200 cm. This was done to prevent any boundary contamination to affect the region of interest. Figure 2 shows the computational domain for the 100 cm calculation.

The initial number density was taken as 15 torr; the shot energy was 200 MJ (the standard TDF base case). The present code does not model ion deposition; therefore, MF-FIRE[5] was used to generate the initial ion temperature profile. Figure 3 shows this profile. Also indicated in the figure is the region where the shock is "launched": when the hydrodynamic speed is greater than the diffusion speed. The distance between the He region and the target was varied in this investigation; the three values are also shown in the figure (10, 40, and 100 cm). These were chosen to be inside the initial high energy deposition region (10 cm), just beyond it (40 cm), and prior to launching the shock (100 cm).

The present investigation was not concerned with detailed modeling of the nitrogen-helium interface. Thus, the computer code considered only a single species; the helium region was just modeled as nitrogen with negligible opacity (transparent gas). Essentially, the helium region served as a pseudo-boundary condition for the nitrogen region. Only the pressure loading in the nitrogen region (radial and downward axial) were of interest.

1.1 100 cm

The first calculation positioned the interface 100 cm above the target. This allowed sufficient time for the fireball to form before it encountered the He region. Figure 4 shows the development of the fireball. One can note that it has just begun to interact with the He at 17 microseconds. Prior to this time, it has essentially undergone a spherical expansion. At about 32 microseconds, the fireball has become nonspherical due to the change in gas

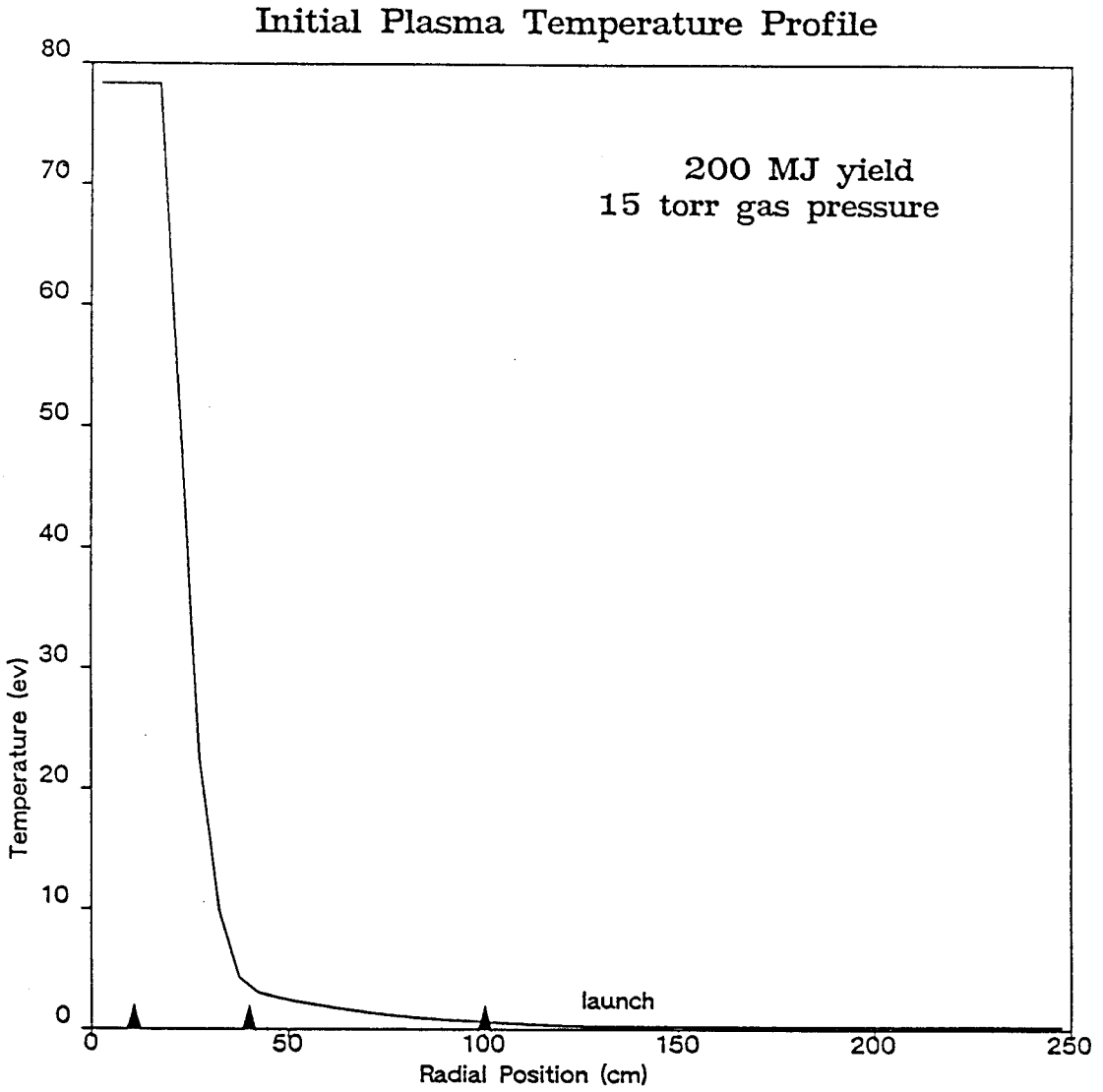

Fig. 3 Initial Gas Temperature Profile

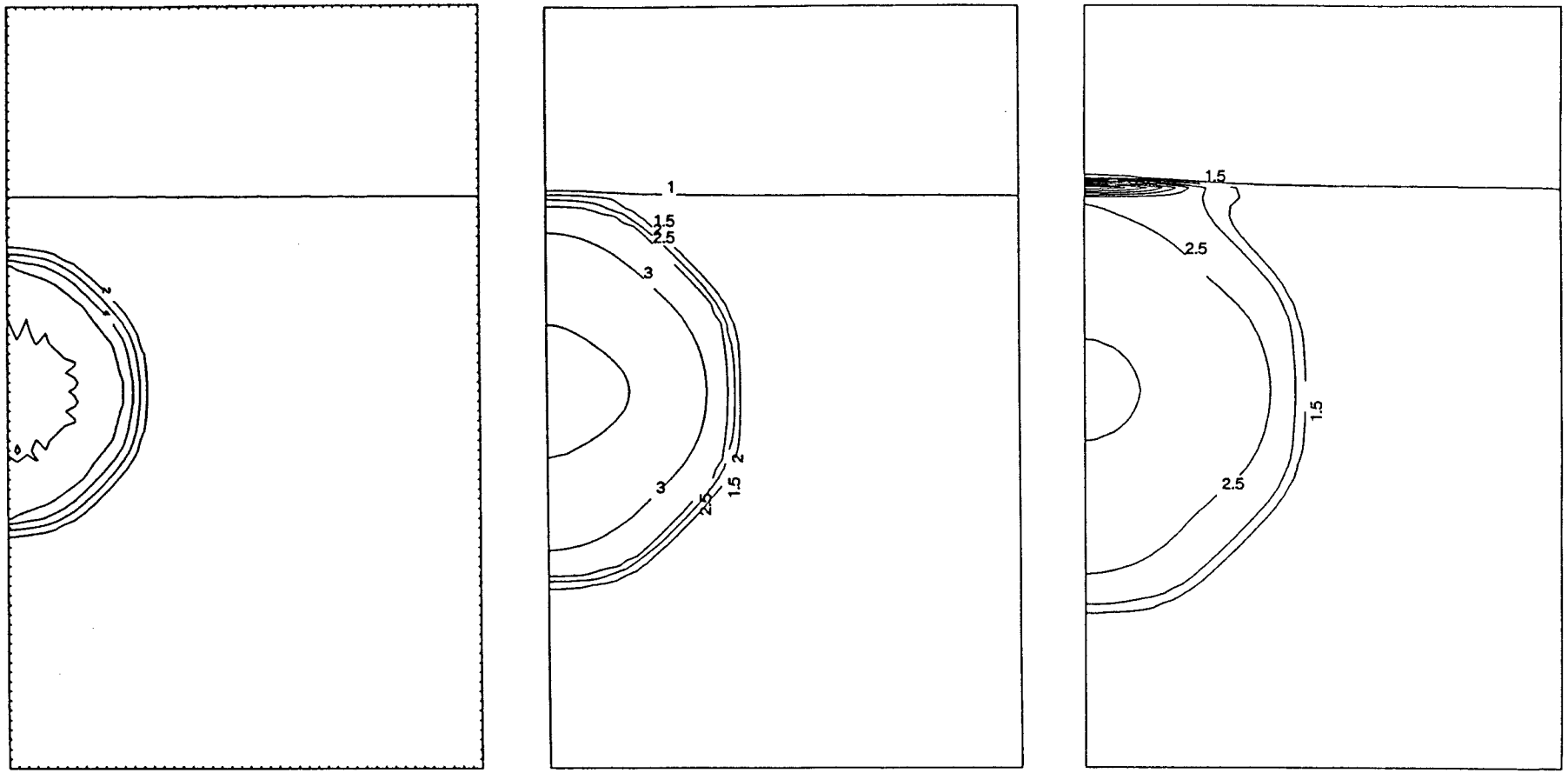

Fig. 4 Gas Temperature Contours for 100 cm. Case

properties at the interface; the effective gas conductivity in the He region is much smaller than the N_2 region due to the small He opacity. Therefore, on the time scales illustrated, the thermal wave does not propagate into the He region. Figure 5 illustrates an interesting effect of this opacity discontinuity: the gas temperature in the first He zone increases rapidly. This is due to the rapid compression of the He from the high stationary pressure gradient at the interface. The propagation of the thermal wave is dominated by the energy exchange between the radiation and the plasma fields; this exchange does not take place in the He region due to the pure transparent assumption. Finally, Fig. 6 illustrates the spatial distribution of the radiation temperature after the fireball has reached the interface. Here we can see that the radiation field has "burst" into the He gas and the fireball is venting energy "upward" in the cavity. One will note that the radiation temperature is approximately 2.5 eV at this point. This will be a crucial value in determining the effectiveness of this pressure reduction scheme.

Figure 7 shows the comparison between the vented 100 cm case and a single region nitrogen case. Essentially there are only minor differences. This is due to the relatively low radiation interface temperature when the fireball reaches the He. Since the radiation energy density is proportional to the fourth power of temperature, the actual energy flux being vented out of the fireball is comparatively small. Thus, the effect on the overpressure would be negligible.

1.2 40 cm

In an effort to increase the interface radiation temperature when the fireball reaches the He region, the separation distance was reduced from 100 cm to 40 cm. Figure 8 shows the ion and radiation temperatures along the

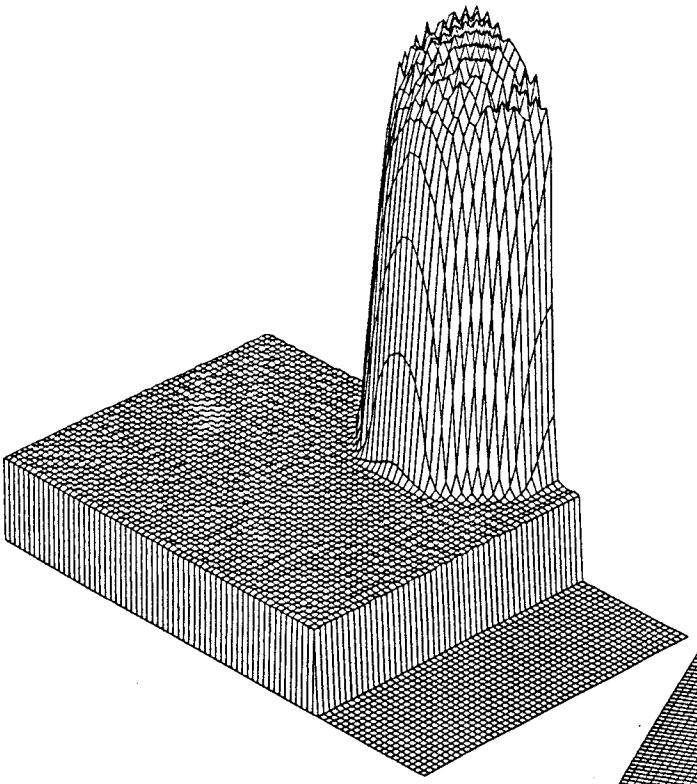

Plasma TemPerature t = 2 e-06 s

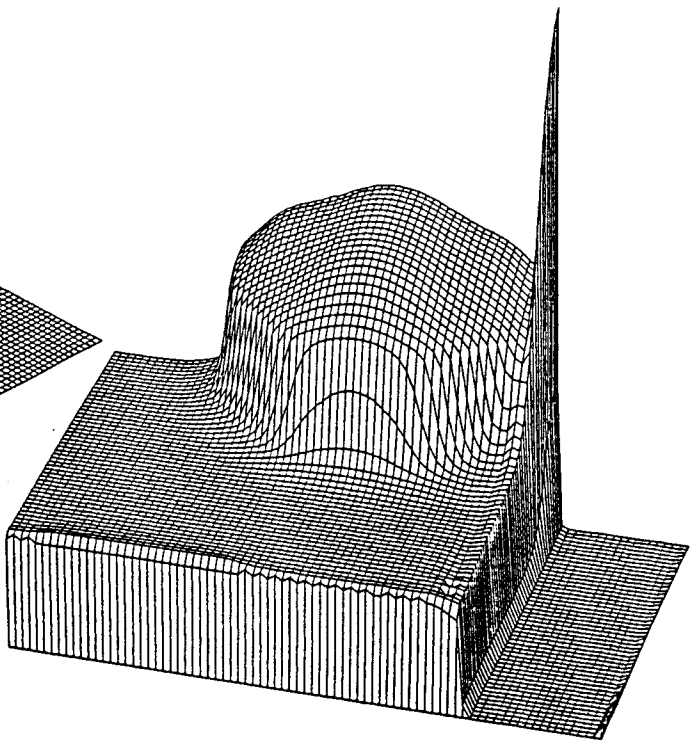

Plasma Temperature 3.17e-5 s

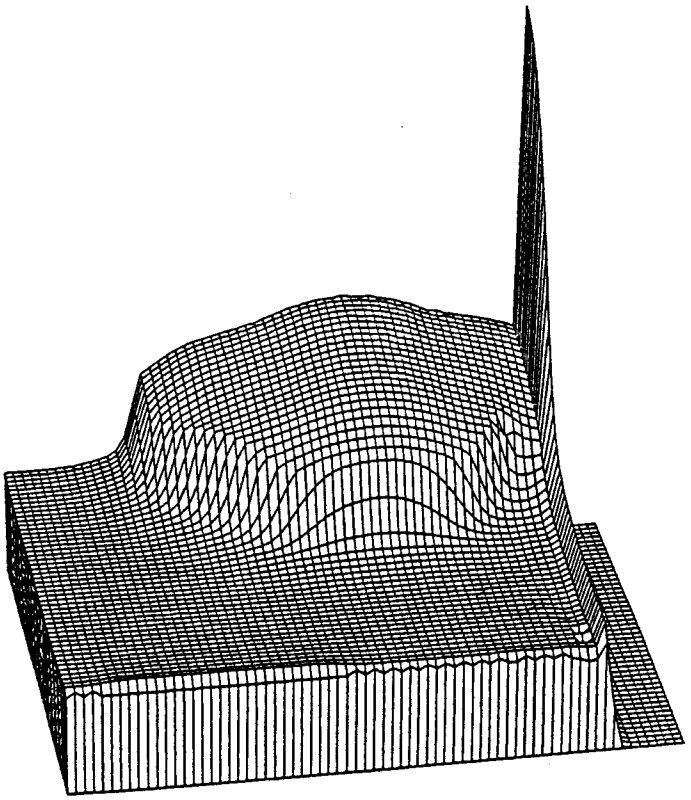

Plasma Temperature (100cm) 44.5e-6s

Fig. 5 Gas Temperature for 100 cm. Case

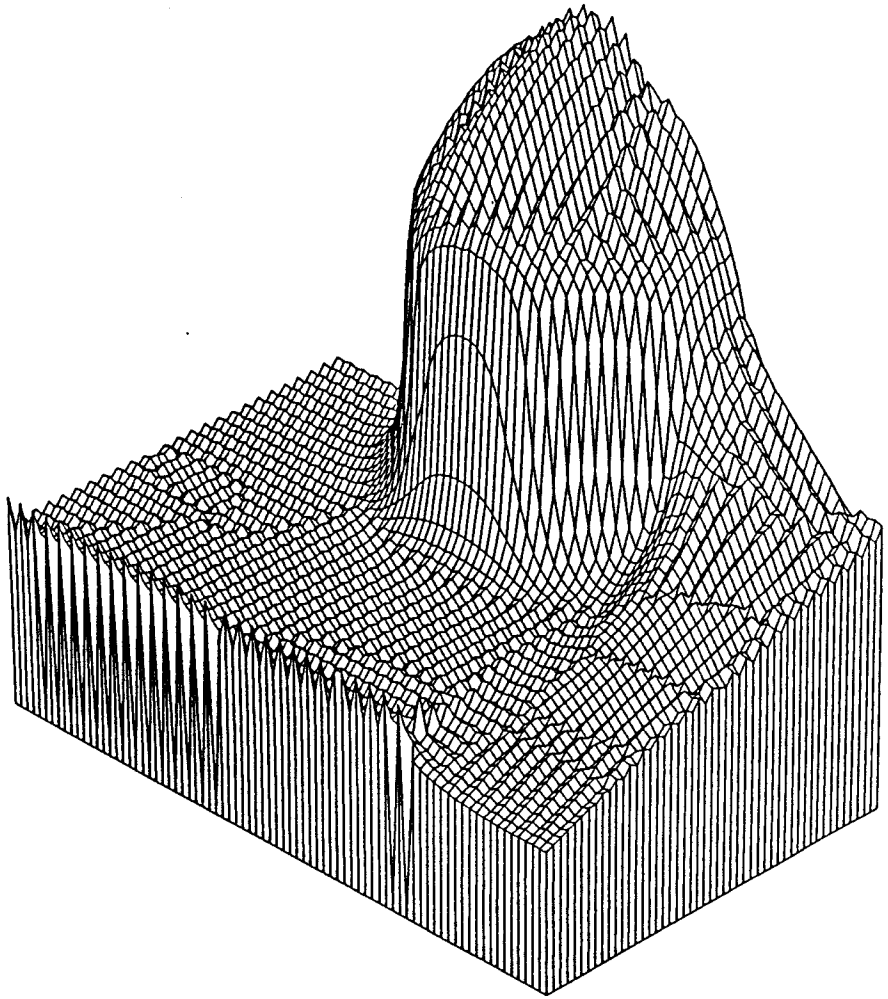

Radiation Temperature 2.16e-5 s

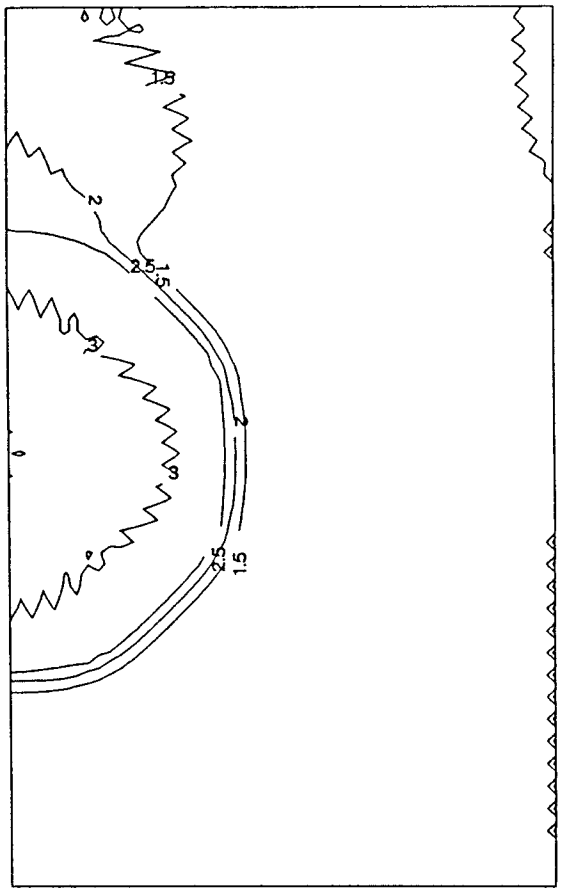

Radiation Temperature 2.16e-5 s

Fig. 6 Radiation Temperature for 100 cm. Case

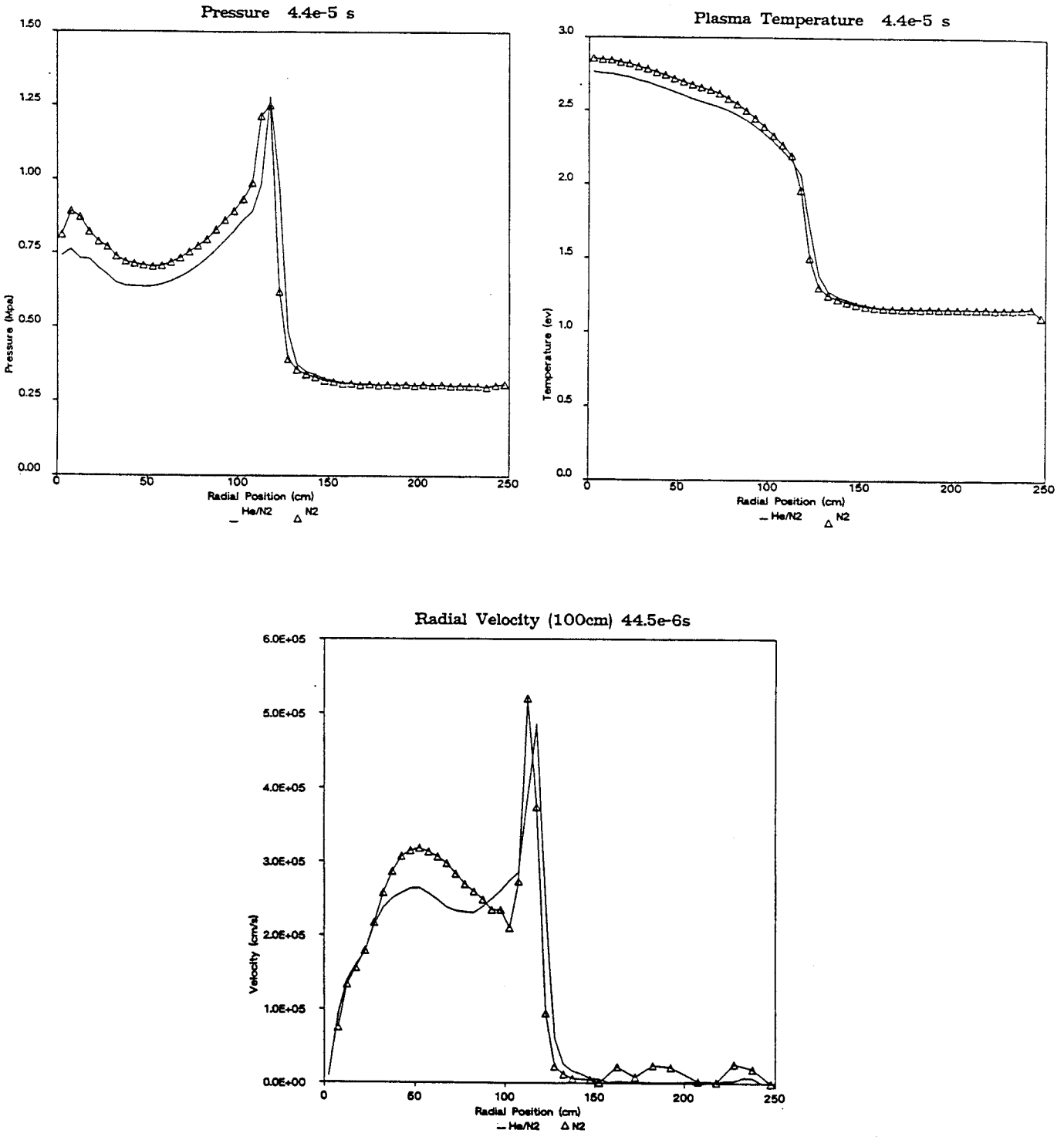

Fig. 7 Comparison of Pressure, Gas Temperature and Velocity between the vented 100 cm. case and std. nitrogen calculation (radial direction from target).

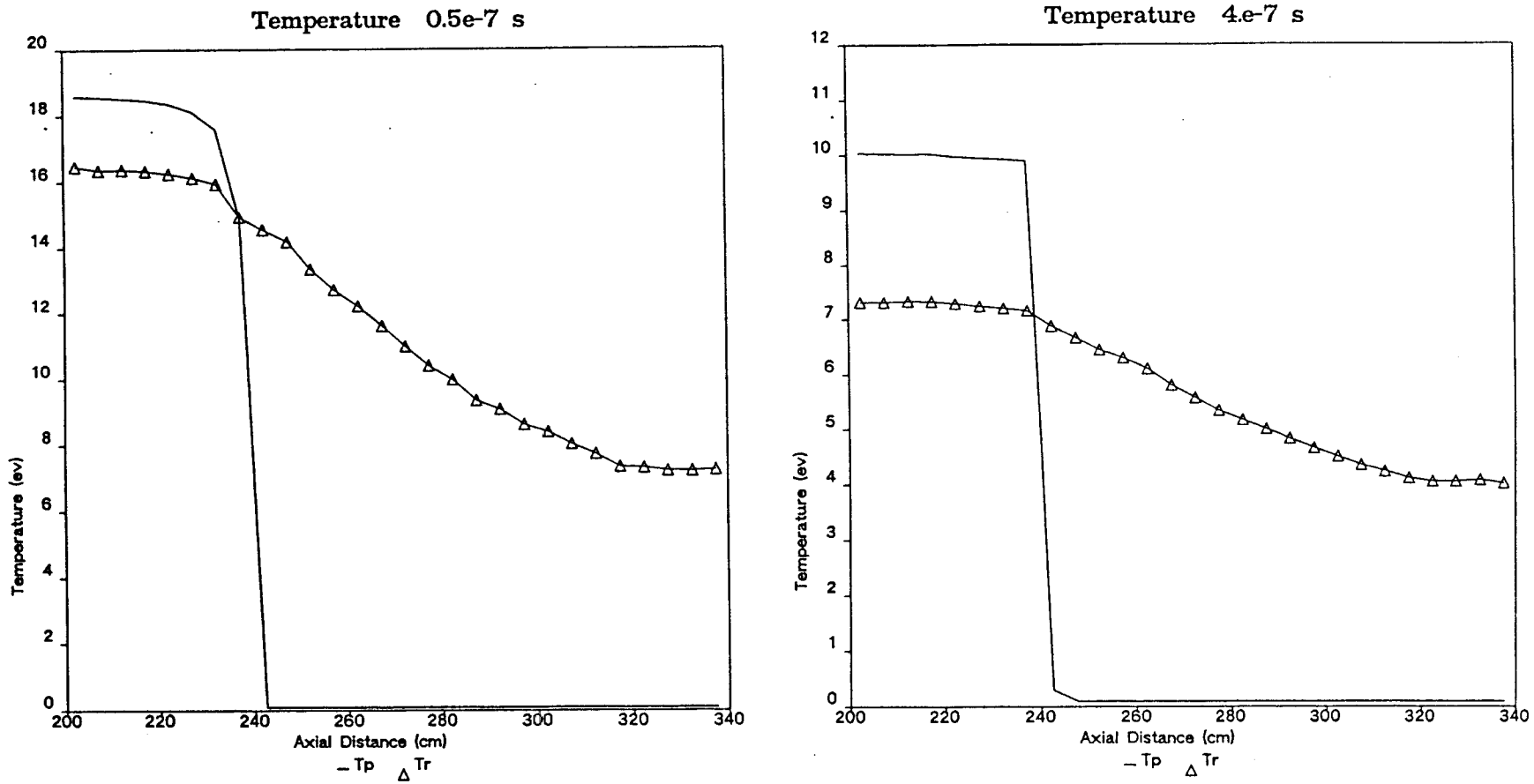

Fig. 8 Gas and Radiation Temperatures in Axial Direction (upward) for 40 cm. case (target at 200 cm., interface at 240 cm.)

vertical axis for two early times. The target was at 200 cm and the interface located at 240 cm. Here we see that the interface radiation temperature is much higher than the 100 cm case when the fireball reaches the helium. A temperature of 16 eV results in approximately 1700 times the vented energy flux of the 100 cm case. The spatial behavior of the fireball was otherwise similar to the 100 cm case.

Figure 9 shows the comparison between the 40 cm vented case and the nitrogen case. One interesting point to be made is that the location of the fireball edge, using the location of the maximum velocity, is the same for both calculations. This will simplify the analysis in Section 2. One can easily see that the vented fireball contains less energy due to the reduced core ion temperature and velocity. However, the peak velocities are similar because they are essentially determined from the pressure gradient at the edge of the fireball, which are about the same for both calculations. The pressure gradient, or equivalently the temperature gradient in the diffusion dominated region, is determined by the opacity variations of the cavity gas. Thus, one would expect the gradients to be similar irrespective of the venting process.

1.3 10 cm

The final calculation reduced the distance between the target and the He region to 10 cm. This was done to determine the maximum realistic effect of energy venting. Figure 10 shows the ion and radiation temperatures along the vertical axis during the initial stages of the fireball evolution. Here, one can easily see the interaction of the He region with the formation of the fireball. One interesting point is that the radiation temperature quickly reaches an equilibrium value of about 7 eV while the plasma temperature remains somewhat higher (12 eV); the energy loss by venting is balanced by the

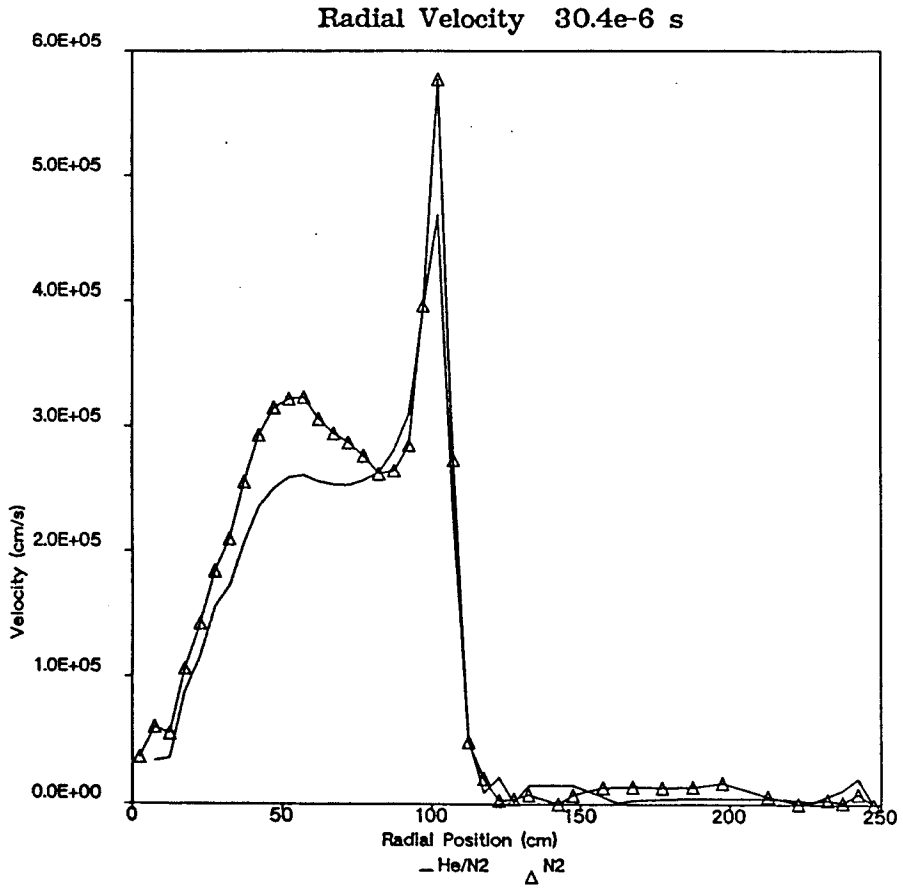

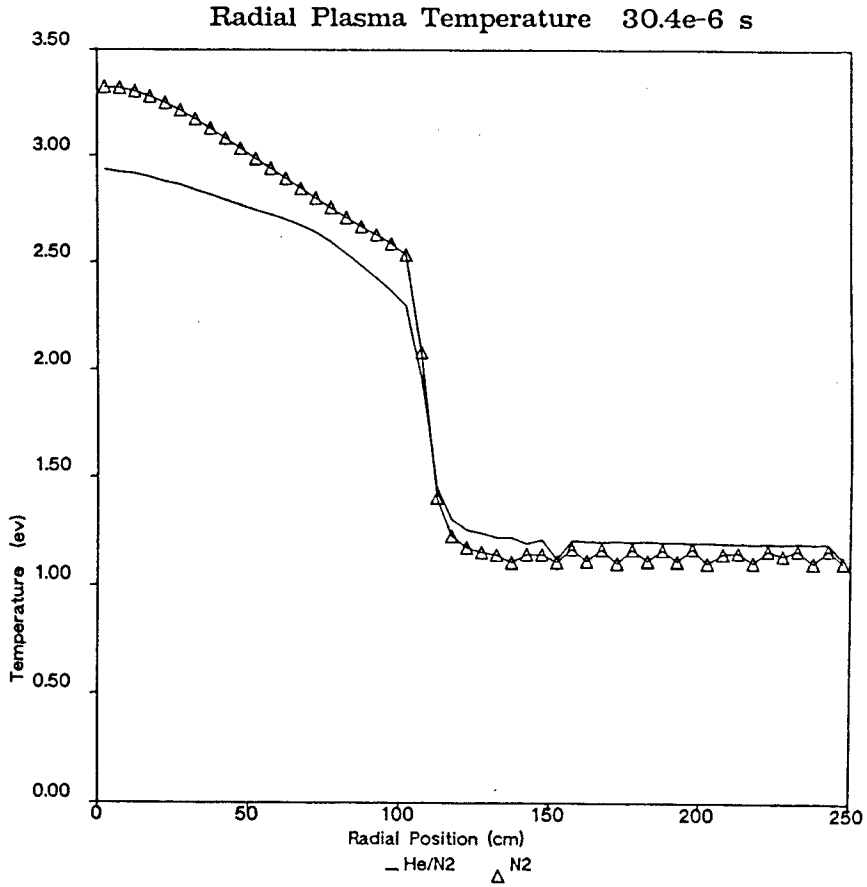

Fig. 9 Comparison of Velocity and Gas Temperatures between vented 40 cm. case and pure nitrogen (radial direction from target)

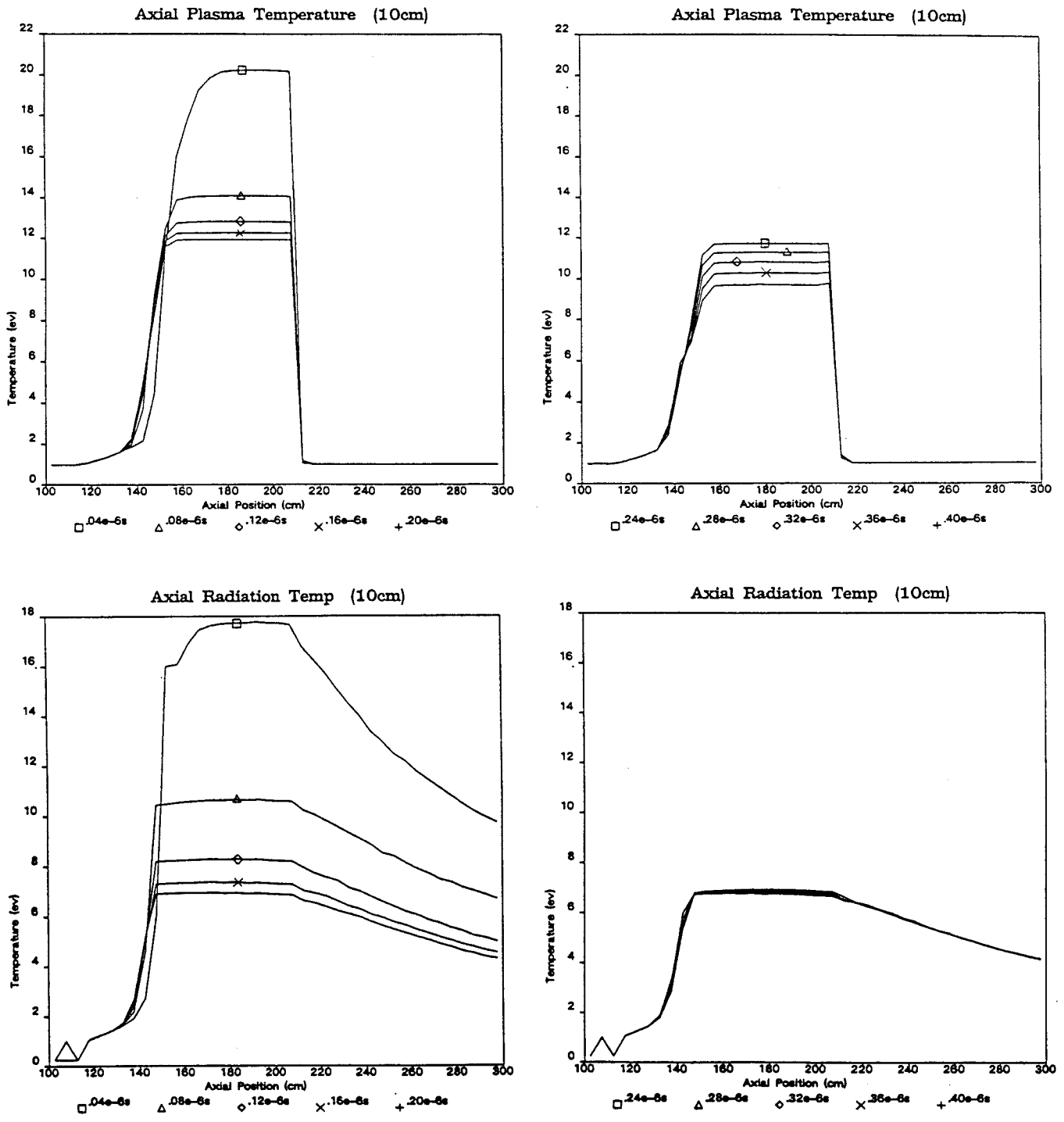

Fig. 10 Axial Gas and Radiation Temperatures for 10 cm. case (target located at 200 cm., interface at 210 cm.)

radiation emission from plasmas. These values are determined by the opacity differences in the parameter space of interest (temperatures and number densities). This equilibrium radiation temperature limits the vented energy loss. A different gas or fluid conditions might yield a more favorable equilibrium temperature.

As mentioned earlier, the diffusion approximation was used to model the radiation transport. This assumption is not valid in the He region, and in fact, "contaminates" the radial region at the target level. Figure 11 illustrates this effect. The contour plot shows the non-physical propagation of the radiation temperature in the He region. One would expect little radial diffusion as the radiation is transported upward from the "hole", the interface zone. However, the diffusion approximation with a scalar effective diffusivity causes the large radial propagation. The radiation then reenters the nitrogen region and interacts with the plasma, increasing its energy. This results in a diffuse region near the interface and is illustrated in the perspective plot of the plasma temperature. One can contrast the sharp gradient temperature along the downward axial direction to the gentle slope in the radial direction. This is entirely an artifact of the computational models used. For this reason, comparisons between the pure nitrogen calculation were done using the fluid values along the downward axial direction from the target, unaffected by this interface problem. Figure 12 shows this comparison. One can observe that although the peak stagnation pressure is essentially the same for both cases, the core values are noticeably reduced. The same trends are seen in the total energy density (internal + kinetic + pressure). However, the total fireball energy depends on the volume integral of this quantity and the majority of the volume of a sphere is in its outer radius. The

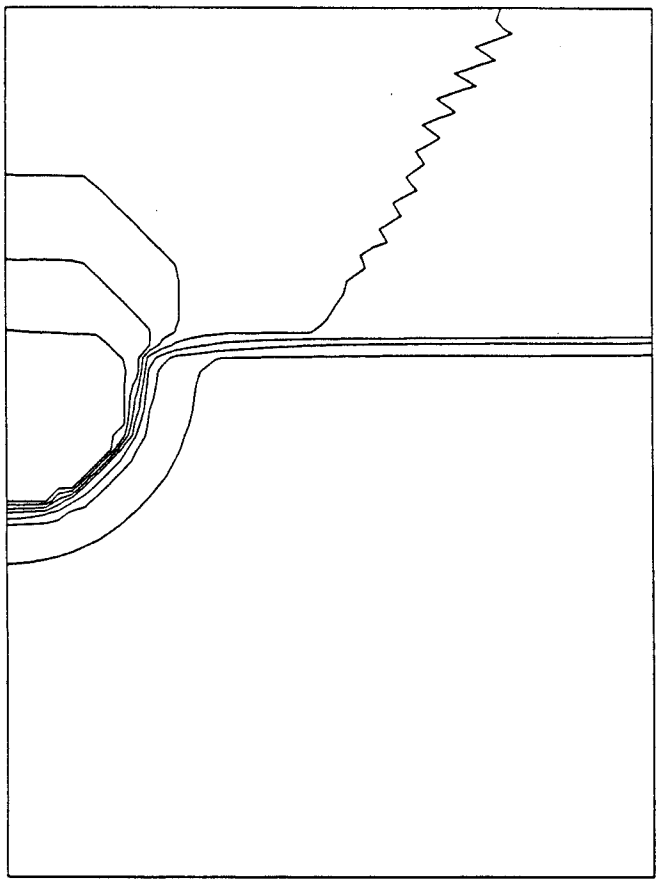

Radiation Temperature (10cm) 0.1e-6s

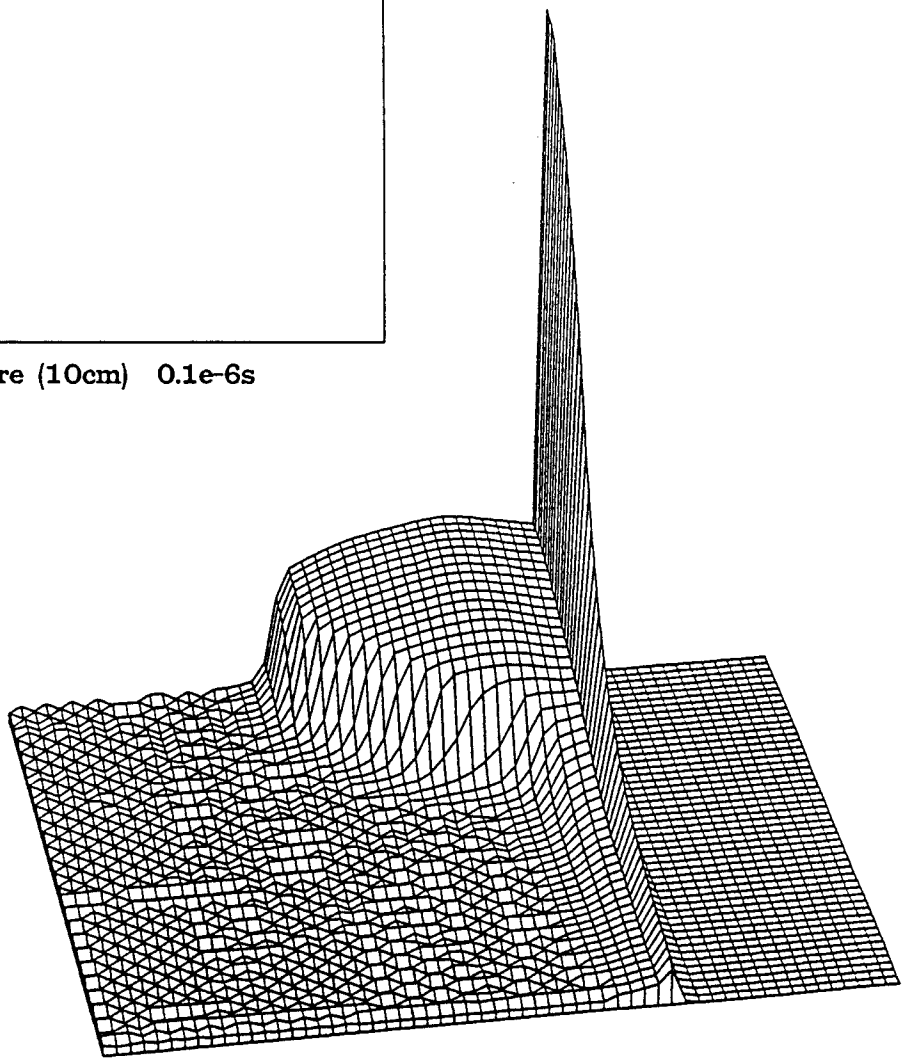

Plasma Temperature (10cm) 16.9e-5s

Fig. 11 Gas and Radiation Temperatures for 10 cm. case.

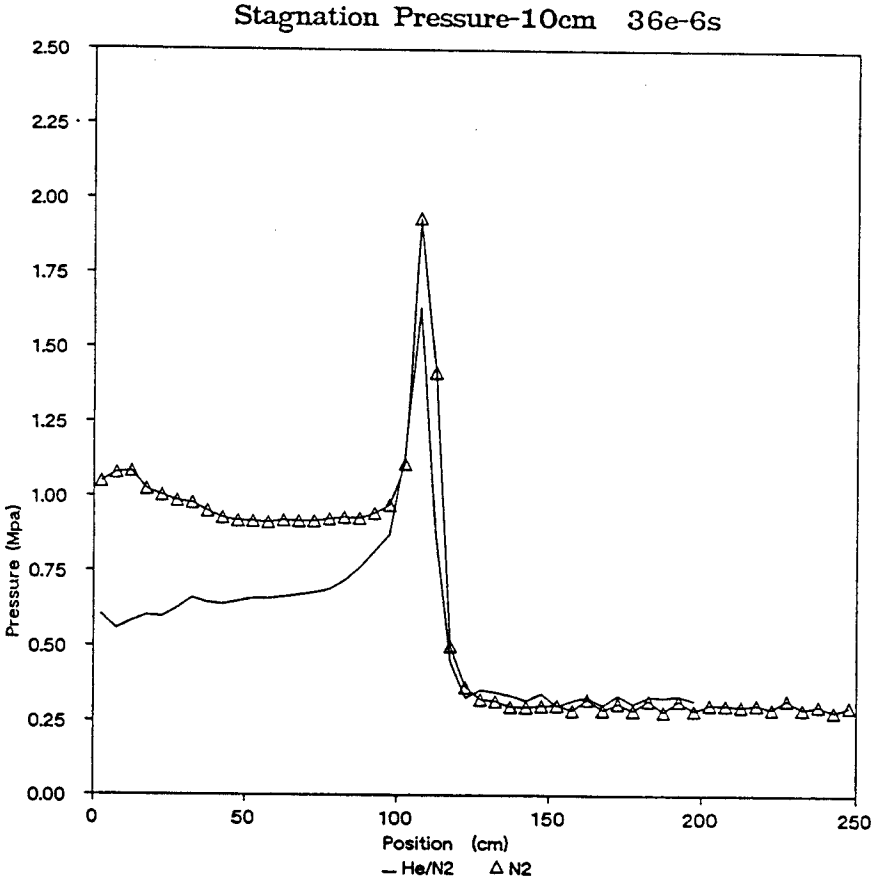

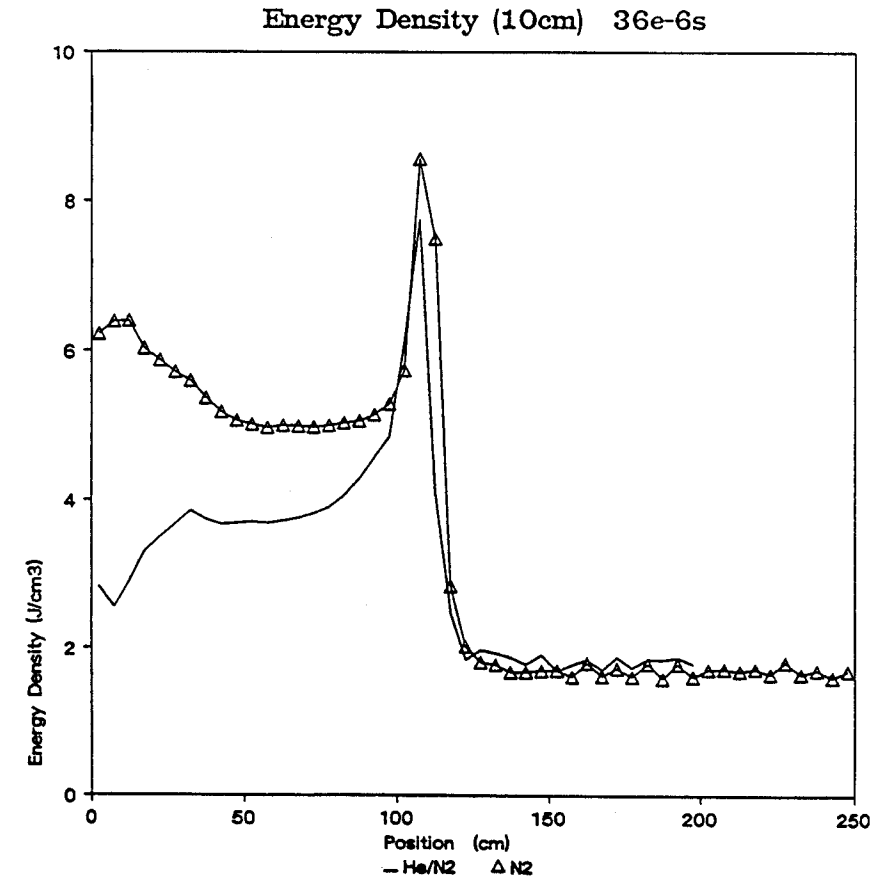

Fig. 12 Comparison between Stagnation Pressure and Total Energy Density between the vented 10 cm. case and pure nitrogen case. (axial downward, target at 0 cm.)

differences are not as great as the plots would tend to indicate. This will be discussed in the following section.

2. Analysis

Figure 13 clearly shows the effects of the venting for the base conditions used. Here the energy in a pseudo-uniform fireball whose radial profile is the vented case (an equivalent target yield) is scaled to a single region expansion. One can see that the 100 cm separation distance resulted in only a minimal effect while the 10 cm case achieves a reduction of approximately 20%. Since the radial position of the fireball is similar for both the vented and non-vented cases, it is easy to determine the overpressure reduction one would expect. Strong shock theory[6] states that the pressure impulse is proportional to the total energy and inversely proportional to the radius cubed. However, for the same radius, the impulse ratio between the vented and non-vented cases simply reduces to the ratio of the fireball energies. Thus, Fig. 13 gives the impulse reduction directly.

Figure 14 shows the temporal interface radiation temperature behavior for the three cases; it is equivalently the vented energy flux. This figure helps to interpret the results of the preceding figure. We can see that the temperatures for the 10 and 40 cm cases are essentially the same. Thus the differences between the energy ratios is due to the increased vent area for the 10 cm case. The 100 cm interface was too far from the target and thus its vented energy density was too low to significantly affect the fireball.

3. Conclusions and Recommendations

For the TDF base case of a 200 MJ shot and cavity gas pressure of 15 torr, only the 10 cm separation distance resulted in a practical pressure impulse reduction. Its effect was limited by the rapid decrease in the inter-

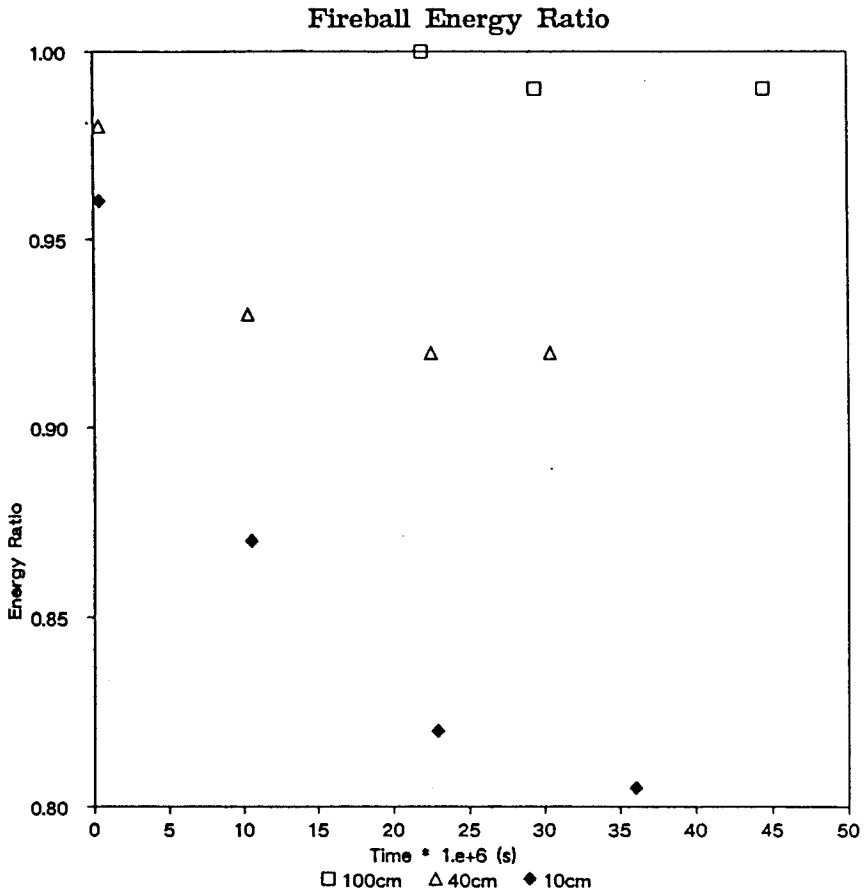

Fig. 13 Ratio of Fireball Total Energy for Vented case to pure nitrogen case.

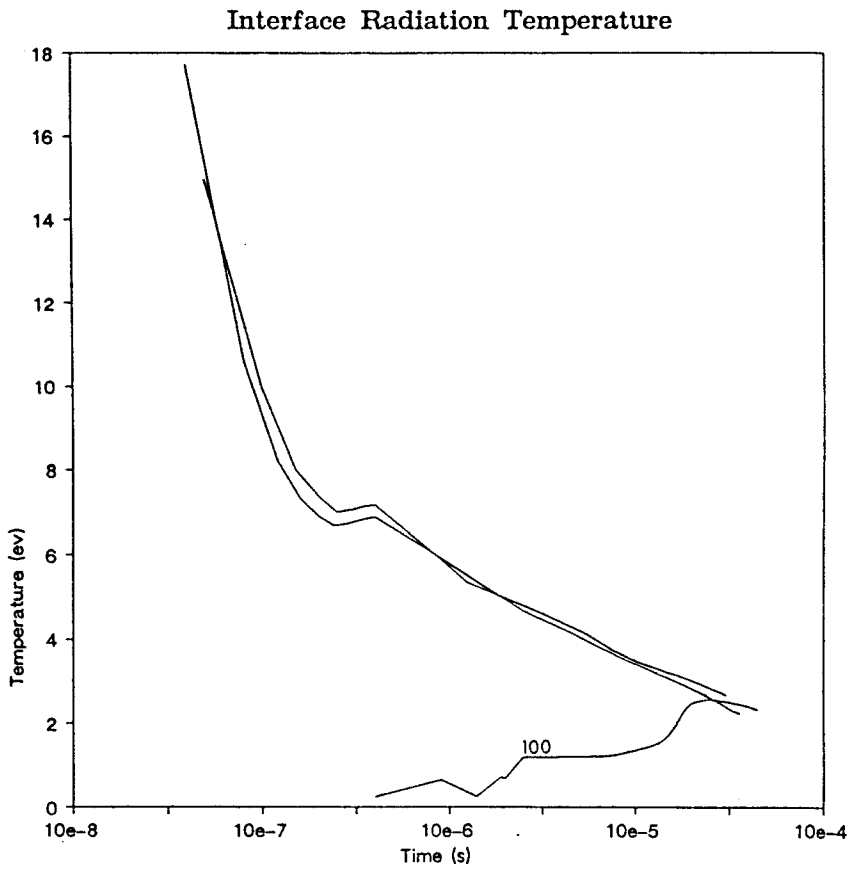

Fig. 14 Radiation Temperature at the He-N_2 interface along z-axis for 10, 40, and 100 cm. cases.

face radiation temperature to an equilibrium value of about 7 eV. The timing of the fireball front remained about the same for both the vented and non-vented cases.

Two free parameters exist which might be varied to increase the venting effect: the shot energy and the cavity gas pressure. Changing the cavity gas pressure would be an attempt to increase the equilibrium radiation temperature and thus increase the vented energy. Increasing the shot energy would increase the duration which energy would be vented before the equilibrium value would be reached. In the present situation for TDF, this would imply performing calculations at a target yield of 800 MJ.

References

1. G.A. Moses, R. Spencer, "Compact-Electron-Beam or Light-Ion-Beam Fusion Reactor Cavity Design Using Nonspherical Blast Waves," Nucl. Fusion 19, No. 10, 1386-1388 (1979).

2. T.J. Bartel, R.R. Peterson, G.A. Moses, "Computer Simulation of a Light Ion Target Explosion in a Stratified Cavity Gas," to be published as a University of Wisconsin Fusion Technology Institute Report.

3. G.C. Pomraning, "Radiation Hydrodynamics," LA-UR-82-2625.

4. R.R. Peterson and G.A. Moses, "MIXERG - An Equation of State and Opacity Computer Code," Computer Physics Comm. 28, 405 (1983); also, University of Wisconsin Fusion Technology Institute Report UWFDM-464 (March 1982).

5. G.A. Moses, T.J. McCarville, R.R. Peterson, "Documentation for MF-FIRE, A Multifrequency Radiative Transfer Version of FIRE," Co puter Phys. Comm. 36, 249 (1985); also, University of Wisconsin Fusion Technology Institute Report UWFDM-458 (March 1982).

6. H.A. Bethe et al., "Blast Wave," LA-2000 (August 1947).